*Inorg. Chem.* **2008**, *47*, 11958−11964

# Real-Space Pairing through Charge Transfer Excitons in High-$T_C$ Cuprates

**Michel Pouchard,* Jean-Pierre Doumerc, and Antoine Villesuzanne**

*CNRS, Université de Bordeaux, ICMCB, 87 Av. Dr. A. Schweitzer, Pessac, F-33608, France*

Received July 7, 2008

While approaching a Mott−Hubbard transition by hole doping of the pristine $La_2CuO_4$ cuprate, excitons are created because of exciton−exciton and exciton-doping hole stabilizing interactions. Here, excitons are of charge-transfer Frenkel-type, with effective $Cu^+O^-$ electrical dipoles that solvate the doping charges. Assuming a moderate screening by charge carriers, we show that mobile exciton-solvated doping holes should be associated in pairs either by a deep energy well or as thermodynamically stable pairs that can glide in the [100] or [010] direction after Bose condensation. Exciton−exciton dipolar interactions constitute thus the "pairing glue" in this model, which is based on instantaneous interactions and intrinsically differs from the previous excitonic models, in which BCS virtual phonons were replaced by virtual excitons.

## 1. Introduction

As pointed out by several physicists in the 1960s (see, for example, ref 1 and references therein) and following Mott's pioneering ideas,[2] electrons and holes at the Fermi level of a semimetal (formed through a Mott−Hubbard transition) can condense into a less conducting excitonic phase. We recently pointed out[1]that such a situation may describe hole-doped high-$T_C$ cuprates.

Metallic behavior shrinks the cell parameters, increases the copper−oxygen bond covalency and orbital overlaps, thus destabilizing the lower Hubbard band (LHB) of oxygen parentage and stabilizing the upper Hubbard band (UHB) of copper parentage.[1] As the LHB-UHB gap narrows or even closes, a charge transfer (CT) occurs from the strongly antibonding top of the LHB toward the non-bonding bottom of the UHB. We assumed that, after an avalanche-type process,[1] an equilibrium is reached:

$$O^{2-}(\mathrm{LHB}) + Cu^{2+} \rightleftarrows O^-(h^+_{CT}) + Cu^+(e^-_{CT}) \qquad (\Delta H)$$

The $h^+_{CT}$ holes and $e^-_{CT}$ electrons may condense as Frenkel-type excitons localized on first-neighbor oxygen and copper atoms. An excitonic phase is thus formed, with a strong stabilizing interaction between doping holes and excitons electrical dipoles. This should result in a strong trapping of charge carriers; our assumption of exciton formation (exciton is taken here in a broad sense) is based on previous theoretical as well as experimental considerations such as the following:

(i) Theoretical studies by Halperin and Rice,[3] des Cloizeaux,[4] Jérome, Rice and Kohn[5] of a Mott−Hubbard transition from an insulator to a semimetal, predicting the existence of an intermediate excitonic insulating phase along with variations of physical or chemical pressure.

(ii) The theoretical work by Hirsch and Scalapino,[6] published 1 year before the discovery of high-$T_C$ superconductivity by Bednorz and Müller,[7] and entitled "Excitonic mechanism for superconductivity in a quasi-one-dimensional system".

(iii) The work of Varma, Schmitt-Rink, and Abrahams[8] entitled "Charge transfer excitations and superconductivity in ionic metals".

(iv) Some experimental results such as those of Chakraverty, Sarma, and Rao[9,10] showing, by X-ray photoelectron spectroscopy, the occurrence of large quantities of $Cu^+$ and $O^-$ species in various high-$T_C$ cuprates, or the numerous

* To whom correspondence should be addressed. E-mail: pouchard@icmcb-bordeaux.cnrs.fr. Phone.: +33 540 008 459. Fax: +33 540 002 761.

(1) Pouchard, M.; Doumerc J.-P.; Villesuzanne, A. *Inorg. Chem.* **2008**, *47*, 8487.
(2) Mott, N. F. *Philos. Mag.* **1961**, *6*, 287.
(3) Halperin, B. I.; Rice, T. M. *Rev. Mod. Phys.* **1968**, *40*, 755, and discussions following the paper presentation.
(4) Des Cloizeaux, J. *J. Phys. Chem. Solids* **1965**, *26*, 259.
(5) Jérome, D.; Rice, T. M.; Kohn, W. *Phys. Rev.* **1967**, *158*, 462.
(6) Hirsch, J. E.; Scalapino, D. J. *Phys. Rev. B* **1985**, *32*, 117.
(7) Bednorz, J. G.; Müller, K. A. *Z. Phys. B: Condens. Matter* **1986**, *64*, 189.
(8) Varma, C. M.; Schmitt-Rink, S.; Abrahams, E. *Solid State Commun.* **1987**, *62*, 681.



10.1021/ic801266q CCC: $40.75 
Published on Web 11/18/2008

**Table 1.** Total Energy $U_n$ Gained by an Excitonic System of $n$ Excitons[a]

| $n$ | 1 | 2 | 3 | 4 | 5 | 6 | $n\rightarrow\infty$ | $n, m$ | 1, 2 |
|---|---|---|---|---|---|---|---|---|---|
| $-U_n$ | 720 | 1680 | 2664 | 3655 | 4649 | 5644 | 998 × n | $-U_{12}$ | 2612 |
| $-E_n$ | | 240 | 504 | 775 | 1049 | 1324 | 278 × n | $-E_{12}$ | 452 |
| $-E_n/n$ | | 120 | 168 | 194 | 210 | 221 | 278 | $-E_{12}/3$ | 151 |

| $n$ | $-U_{nn}$ | $-U_{2n}$ | $U_{nn} - U_{2n}$ | $-2 \times U_n$ | $U_{nn} - 2U_n$ | $-E_{nn}$ | $-E_{nn}/n$ | $(U_{nn} - 2U_n)/2n$ |
|---|---|---|---|---|---|---|---|---|
| 2 | 3233 | 3655 | +422 | 3360 | +127 | 353 | 88 | +31.8 meV |
| 3 | 5173 | 5644 | +471 | 5328 | +155 | 853 | 71 | +25.8 meV |

[a] $E_n$: exciton-exciton interaction; $E_n/n$: specific interaction per exciton. Top: values (in meV) for linear $I_n$-type chains as well as for a $L_{12}$ bent chain ($n$=1, $m$=2). Bottom: values for double chains (cell parameter $a$ apart)..

observations of humps in the conductivity vs temperature curves (see, for example, ref 11), immediately above $T_C$, in agreement with a semiconducting behavior arising from a charge-transfer excitonic phase before Bose condensation.

(v) Recently, Gedik et al.,[12] using ultrafast crystallography, revealed a photoinduced phase transition in oxygen-doped $La_2CuO_4$, corresponding to a large increase of the $c$ lattice parameter, suggesting that the excitation pulse induces a charge transfer of exciton type from $O^{2-}$ to $Cu^{2+}$, in the $CuO_2$ planes.

In addition, the recent real-space observations by Hanaguri et al.,[13] Kohsaka et al.,[14] and Pasupathy et al.,[15] by tunneling-asymmetry electron−hole excitations demonstrated the importance of nanometric inhomogeneities in the carrier distribution on oxygen atoms, as well as in the superconducting gap values. Structural and chemical inhomogeneity affects the excitations of both the normal and the superconducting states; pairing is preserved few tens of degrees above $T_C$ and anticorrelations do exist between the gap values and the conductance in the normal state. Our charge-transfer excitonic model, with various exciton topologies and attractive effective interactions, provides possible explanations for all these observations.

Moreover, we proposed that large dipole−dipole interactions are able to provide the "glue" between such exciton-solvated doping hole (ESH) entities. The aim of this paper is to examine these various interactions, particularly focusing on two types of ESH dimers, that is, T-type and U-type.

## 2. Energetics of the Excitonic Charge-Transfer Phase

For a single exciton, the CT enthalpy $\Delta H$ can be estimated in an ionic model by the expression:

$$\Delta H = -(EI_2 + AE_2) + |e|\Delta V_M - e^2/d_{Cu-O}$$

where $EI_2$ and $AE_2$ are the copper second ionization energy and the oxygen second electron affinity, respectively, and $\Delta V_M$ is the difference of Madelung potential at Cu and O sites, in the initial phase. The two last terms are the variation in Madelung energy due to the electron transfer (the last term is, too, the binding energy $E_B$ of the formed exciton). In a band model, the closing of the LHB-UHB gap means that $\Delta H$ decreases to zero.

Further energy gain can be obtained by exciton−exciton as well as exciton-doping hole interactions. The magnitude of such interactions can be roughly estimated assuming a compromise between a full CT (+|$e$| on oxygen and −|$e$| on copper) and a strong covalent mixing. The effect of covalency is accounted for by weighting the classical electron−hole electrostatic interaction by a factor $k/\varepsilon_r$ ($k < 1$), where $\varepsilon_r$ is the relative dielectric constant of the medium. Thus, the effective electron−hole interaction associated to the excitonic dipole reads

$$E_B = -\frac{1}{4\pi\varepsilon_o} \times \frac{e^2}{d_{Cu-O}} \times \frac{k}{\varepsilon_r}$$

The same formula holds for the doping hole-effective charge interaction.

In this work, we assumed the value $k/\varepsilon_r = 0.1$. Then, the value of the exciton binding energy is $E_B = -720$ meV.

**2.1. Exciton−Exciton Interactions.** Excitons condense into linear or branched chains in the same way as molecular compounds crystallize through van der Waals forces by alignment of their electrical dipoles. In the following, $I_n$-type will stand for linear rows of $n$ successive excitons and $L_{nm}$-type for bent exciton rows formed by segments of $n$ and $m$ perpendicular entities.

We call $U_n$ (respectively $U_{nm}$) the total energy gained by the excitonic system and $E_n$ (respectively $E_{nm}$) that gained by exciton−exciton interactions only ($E_n = U_n - nE_B$). Table 1 reports $U_n$ and $E_{n(m)}$ calculated values, as well as the exciton efficiency ratio $E_n/n$ for few values of $n$.

Figure 1 shows that the maximum efficiency should be obtained for infinite linear chains ($E_B \times 2\mathrm{Ln}2 - 1 = -278$ meV/exciton). For $L_{12}$-type entities, $E_n/n$ values are, as expected, in between those of $I_2$ and $I_3$ (−151 meV/exciton).

However, it should be mentioned that the screening of the Coulomb potential $V$ by the conducting medium rapidly limits the spatial extent of such chains, according to $V \propto q/r \times \exp(-\lambda r)$, where the screening length $1/\lambda$ can be estimated using the Thomas−Fermi approach. In this limit, and in lightly doped systems, long excitonic chains can be expected.


(9) Chakraverty, B. K.; Sarma, D. D.; Rao, C. N. R. *Physica C* **1988**, *156*, 413.

(10) Sarma, D. D.; Rao, C. N. R. *J. Phys. C: Solid State Phys.* **1987**, *20*, L659.

(11) Grenier, J.-C.; Lagueyte, N.; Wattiaux, A.; Doumerc, J.-P.; Dordor, P.; Etourneau, J.; Pouchard, M.; Goodenough, J. B.; Zhou, J. S. *Physica C* **1992**, *202*, 209.

(12) Gedik, N.; Yang, D. S.; Logvenov, G.; Bosovic, I.; Zewail, A. H. *Science* **2007**, *316*, 425.

(13) Hanaguri, T.; Lupieu, C.; Kohsaka, Y.; Lee, D. H.; Azuma, M.; Takano, M.; Takagi, H.; Davis, J. C. *Nature* **2004**, *430*, 1001.

(14) Kohsaka, Y.; Taylor, C.; Fujita, K.; Schmidt, A.; Lupieu, C.; Hanaguri, T.; Azuma, M.; Takano, M.; Eisaki, H.; Takagi, H.; Uchida, S.; Davis, J. C. *Science* **2007**, *315*, 1380.

(15) Pasupathy, A. N.; Pushp, A.; Gomes, K. K.; Parker, C. V.; Wen, J.; Xu, Z.; Gu, G.; Ono, S.; Ando, Y.; Yazdani, A. *Science* **2008**, *320*, 196.

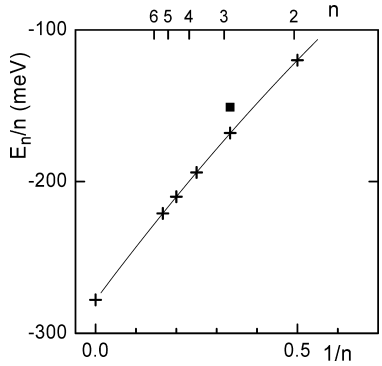


**Figure 1.** Evolution of the specific exciton efficiency, $E_n/n$ (in meV per exciton), with the reciprocal length $1/n$ of the $I_n$-type exciton chain (■: $L_{12}$-type, to be compared with $I_3$).

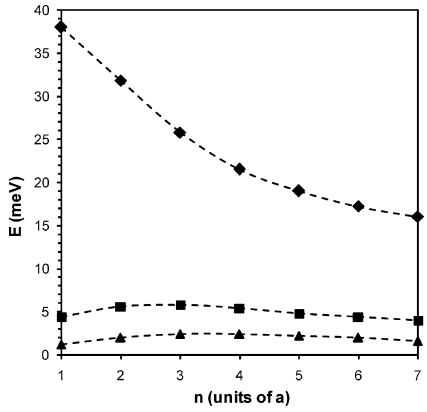


**Figure 2.** Repulsive energy between two parallel rows of $I_n$-type chains as a function of n and of their separation (◆: $a$, ■: $2a$, ▲: $3a$).

For double chains, labeled here I−I, with a separation by the $a$ cell parameter, the total energy $U_{nn}$ is always smaller than the single chain containing the same number ($2n$) of excitons, as shown in Table 1 for $n = 2$ and 3 (as well as $E_{nn}$).

The destabilization arises from two factors: (i) the increase of exciton efficiency with $n$ and (ii) the Coulomb repulsion for close charges of same sign. This last point is illustrated by the difference between $U_{nn}$ and two times $U_n$, which is always positive (Table 1).

Extrapolation to $n = 7$ for various separation lengths $\eta.a$ is displayed on Figure 2. The specific energy ($(U_{nn} - 2U_n)/2n$) decreases smoothly with $n$, but strongly with $\eta$. For $\eta \geq 3$, the specific energy becomes negligible ($\leq$3 meV/exciton).

**2.2. Doping Hole-Exciton Interactions.** A large stabilizing energy is gained from Coulomb interactions between a doping hole, located on an oxygen atom, and an increasing number $n$ of excitons. Table 2 reports the total energy $U_n^+$ of the exciton-charge system and the interaction energy $E_n^+$ (equal to $U_n^+ - nE_B$). $E_n^+$ includes the exciton−exciton interaction energy (dipole−dipole) $E_n$, as well as the charge-exciton interaction $\varepsilon_n^+$. Ratios $E_n^+/n$ and $\varepsilon_n^+/n$ are also given.

Figure 3 shows the evolution of $\varepsilon_n^+$ and $\varepsilon_n^+/n$ as a function of the chain reciprocal length, $1/n$. Table 2 shows that $U_n^+$ increases almost linearly with $n$, while $\varepsilon_n^+$ values saturate toward −500 meV for $I_n^+$-type single chains. As a consequence, $\varepsilon_n^+/n$ decreases slowly with $n$, toward zero.

**2.2.1. $I_n^+$-Type Chains.** As the same screening factor $k/\varepsilon_r$ is used for both doping charges and transferred charges, the $U_n^+$ values do not depend on the position of the doping hole within the chain.

For example, as illustrated in Figure 4a, the hole can be placed in the middle as well as the end of the chain, giving a very simple expression for $\varepsilon_n^+$:

$$\varepsilon_n^+ = E_B \cdot \left(1 - \frac{1}{2} + \frac{1}{3} - \frac{1}{4} + \cdots - \frac{1}{2n}\right)$$

for a chain containing $n$ excitons.

Therefore, as for soliton formation, doping introduces a symmetry element in a non symmetric excitonic chain.

**2.2.2. $I_n$-$I_n^+$-Type Chains.** In this situation, the doping charge ($h_D^+$) is associated to an oxygen atom, in between two copper atoms of the single $I_n$-type chains forming a ladder rung. If the hole is on the first rung, the ESH will be called U-type; if the hole is on another rung, the ESH will be called H-type.

U-type and H-type situations are not energetically equivalent. For example, $U_{22}^+$ and $H_{22}^+$ entities correspond to $\varepsilon_{22}^+ = -610$ meV and $\varepsilon_{22}^+ = -24$ meV, respectively. As a matter of fact, $U_{nn}^+$ entities are always much more stable than $H_{nn}^+$ ones (see section 2.2.4).

Table 2 shows that $\varepsilon_{22}^+$ values are much larger for double chains with the doping hole located in between the chains than for single chains with doping hole inside the chain. Although $\varepsilon_n^+$ is limited to approximately −500 meV for single chains, it can reach values as large as −677 meV for $I_3$−$I_3^+$, revealing much stronger interactions between the charge and its excitonic surrounding.

For high $n$ values, "narrow U-type" entities (Figure 4b) should be considered.

**2.2.3. $L_{nm}$-$L_{nm}^+$-Type Chains.** At this point, we have studied the case $n = 1$, $m = 2$ only. This situation is intermediate between the two previous ones, because the doping hole is located in the middle of the single chain ($I_2^+$) and in between the two legs ($I_2I_2$) (Figure 4c). This topology, called "wide U-type", has the strongest $h_D^+$-exciton interaction energy (−805 meV), even greater than $U_{33}^+$ and $I_6^+$ ESHs.

In the following, we will focus most of our attention on these U-type ESHs.

**2.2.4. Anisotropy of a Double $L_{nm}$-$L_{nm}^+$-Type Chain ($n = 1$, $m = 1$ to 4).** We will consider here the specific Coulomb interaction between the ladder rung $I_2^+$ and two equivalent dipoles of the legs whose position is defined by their number $m$.

Figure 5 shows that (i) interactions are attractive for positive $m$ values (i.e., along the $[0\bar{1}0]$ direction), while they are repulsive in the opposite direction($\bar{m}$); (ii) the magnitude of these interactions decreases rapidly with $|m|$.

These results confirm the instability of $H^+$-type entities, and suggest that the extent of ladder legs could remain limited ($m \leq 3$), in the $[0\bar{1}0]$ direction.

**Table 2.** Interaction Energies (in meV) between a Doping Hole $h_D^+$ and Various Type of Chains [$I_n^+$, $(I_nI_n)^+$, and $(L_{nm}L_{nm})^+$ ($n = 1$, $m = 2$)][a]

| $n$ | 1 | 2 | 3 | 4 | 5 | 6 | $n\rightarrow\infty$ | $n, n$ | 2, 2 | 3, 3 | $n, m$ | 1, 2 |
|---|---|---|---|---|---|---|---|---|---|---|---|---|
| $-U_n^+$ | 1080 | 2100 | 3108 | 4113 | 5115 | 6114 | $499 + 998n$ | $-U_{nn}^+$ | 3843 | 5850 | $-U_{nm}^+$ | 5940 |
| $-E_n^+$ | 360 | 660 | 948 | 1233 | 1515 | 1794 | $499 + 278n$ | $-E_{nn}^+$ | 963 | 1530 | $-E_{nm}^+$ | 1620 |
| $-\varepsilon_n^+$ | 360 | 420 | 444 | 457 | 465 | 470 | 499 | $-\varepsilon_{nn}^+$ | 610 | 677 | $-\varepsilon_{nm}^+$ | 805 |
| $-\varepsilon_n^+/n$ | 360 | 210 | 148 | 114 | 93 | 78 | 0 | $-\varepsilon_{nn}^+/2n$ | 153 | 113 | $-\varepsilon_{nm}^+/(n+m)$ | 134 |

[a] $\varepsilon_n^+/n$ is the specific interaction energy per exciton.

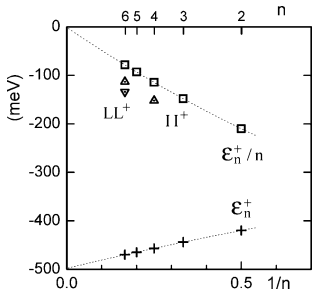


**Figure 3.** Doping hole $h_D^+$-excitons interaction energy $\varepsilon_n^+$ for single chains of $I_n$-type, as well as its specific energy interaction $\varepsilon_n^+/n$ ($\Delta$ and $\nabla$: double chains of $I_n$-$I_n$ and $L_{nm}$-$L_{nm}$ type, respectively).

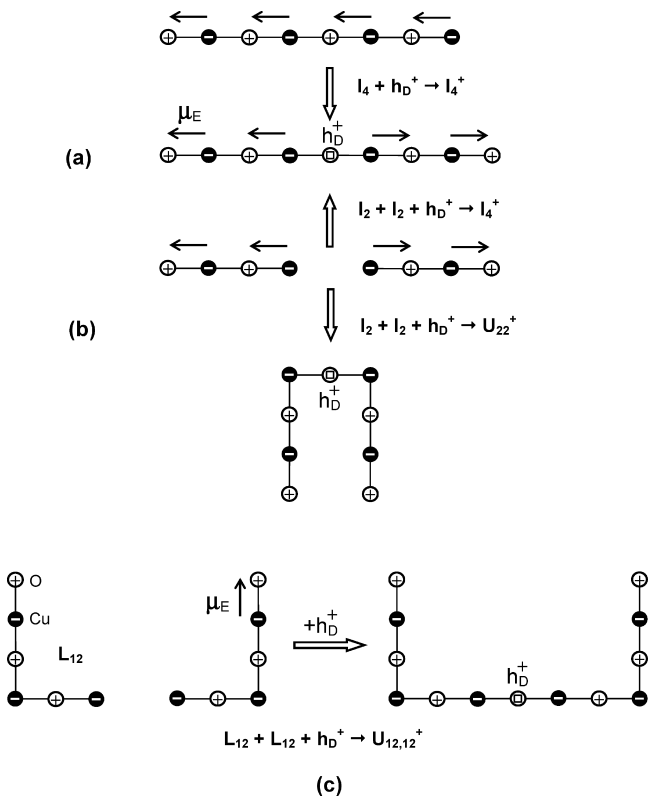


**Figure 4.** Assembly of an $I_4^+$ ESH from (a) two $I_2$ exciton chains and one positive charge or from one $I_4$ chain and a charge. (b) Formation of a $U_{22}^+$ ESH from a parallel double chain $I_2I_2$ and a charge. (c) "Wide" U-type $U_{1212}^+$ entity formation from two $L_{12}$ bent chains and one charge.

**2.3. Charge−Charge ($h_D^+$-$h_D^+$) Interactions.** In an ionic medium with large $1/\lambda$ screening length, $h_D^+$ doping holes are repelling each other. Their Coulomb positive interaction energy is minimized by optimizing their spatial dispersion. The average distance between doping holes depends on the doping rate $x = [h_D^+]$.

For high-$T_C$ cuprates, the superconducting domain extends from approximately $x = 0.06$ to $x = 0.22$, with a $T_C$ maximum for $x \sim 1/6$ (Figure 6). Figure 7 describes the spatial area (number of primitive unit cells) attributed to each doping hole, in the hypothesis of a periodic distribution, for several $x$ values from 1/13 to 1/4. The corresponding range for $h_D^+$-$h_D^+$ shortest distances is 8−14.4 Å. Such distances agree well with the experimental coherence length $\xi$ for Cooper pairs ($\sim$ 10 Å in the *a*-*b* plane) in high-$T_C$ cuprates, and with our assumption of screening length $1/\lambda$.

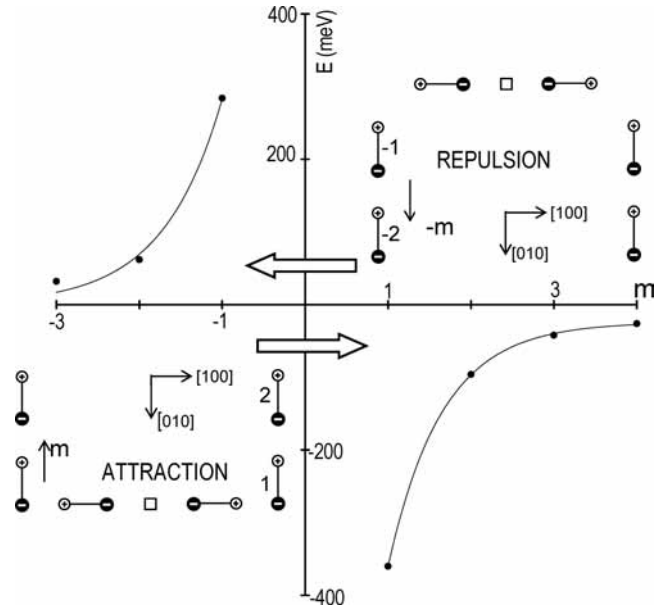


**Figure 5.** Interaction between $I_2^+$-type ESH, forming one rung of an exciton ladder, and two equivalent excitons of its legs depending on the position of the exciton-pair, denoted by their $m$ position number along [0$\bar{1}$0] and $\bar{m}$ along [010].

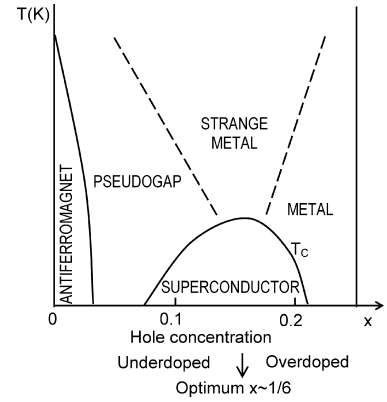


**Figure 6.** Schematized phase diagram for $A_2CuO_{4+\delta}$ (A = La, Sr) showing the superconductivity composition range (adapted from ref 14).

## 3. Attractive Interaction between Two ESHs

Although doping charges repel each other, we claim that an effective attractive interaction can be achieved between two ESHs.

We will examine the possible formation of dimers (two associated ESHs) by means of a net attractive interaction.

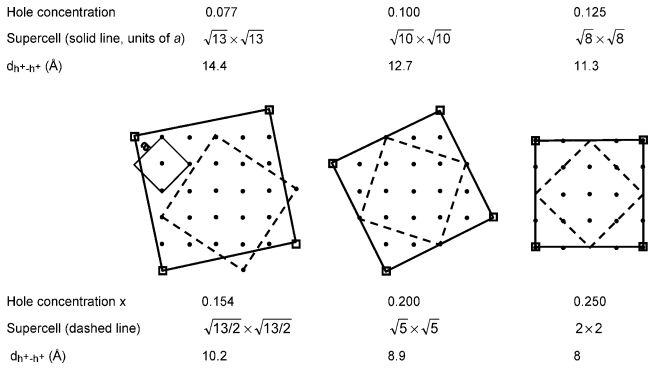


**Figure 7.** Possible ordered dispersion of the doping holes in a $CuO_2$ layer depending on the hole concentration $x$. Only oxygen atoms are represented, as well as the superstructures in units of cell parameter $a$. The maximum interhole distance $d_{h+-h+}$ is indicated.

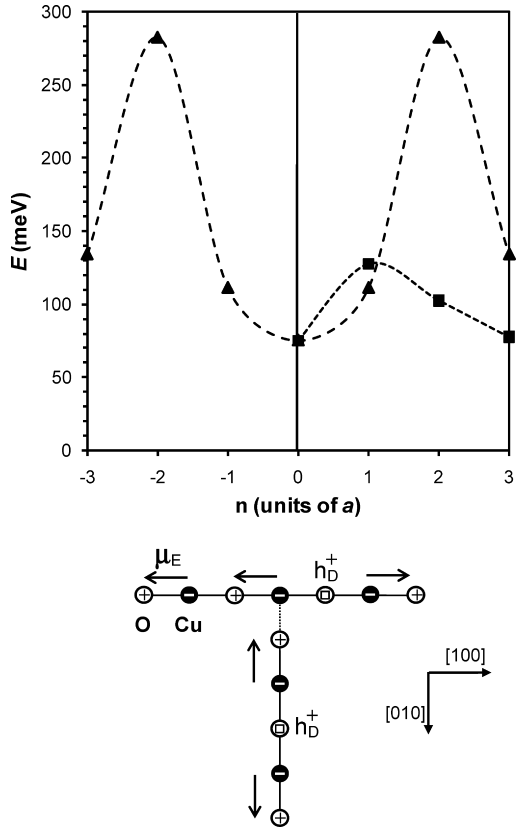


**Figure 8.** Coulomb interaction between two $I_n^+$-type ESH monomers ($I_2^+$ and $I_3^+$) approaching in a perpendicular manner and depending on their mutual position along [100] (▲) and [010] (■). The formation of a $T_{32}^{+2}$ -type dimer is unstable versus an infinite dilution of the two monomers, but an activation energy is required to break the pair.

Two situations can be envisaged: (i) a thermodynamically stable association with total energy, labeled $U_{nm}^{+2}$, smaller than the sum of the two monomer energies, or (ii) the existence of a deep energy well that keeps the monomers from separating, especially at high doping rates.

**3.1. Single chain $I_n^+$-type ESHs: T-type dimers.** As previously shown,[1] this type of interaction scheme leads to a net positive energy. However, most of T-type configurations obtained by approaching $I_n^+$-type ESHs in a perpendicular manner present energy wells of various depths.

Figure 8 describes the formation of a $T_{32}^{+2}$-type dimer, for which $U_{32}^{+2} = -5134.5$ meV, which is less stable than

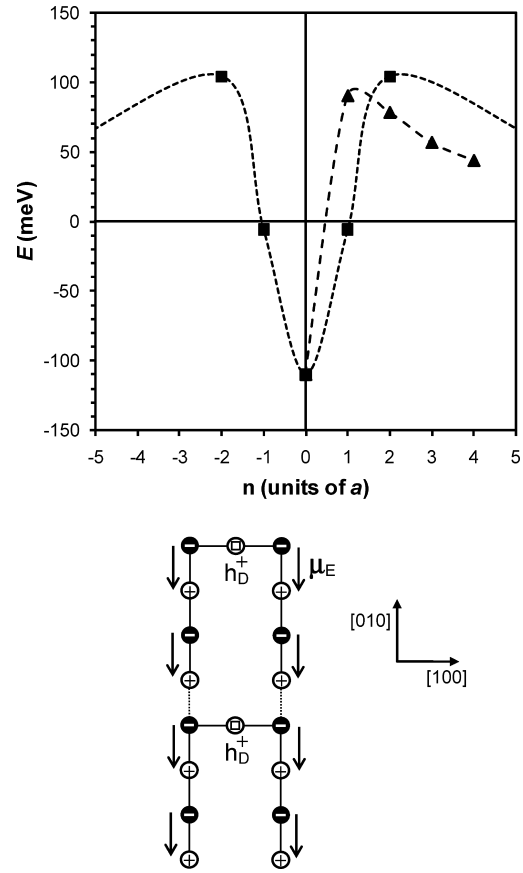


**Figure 9.** Approach of two $U^+$-type ESH as in Figure 8. The $U^{2+}$ dimer is thermodynamically stable and corresponds thus to the ground state. The dimer configuration lies in a 200 meV-deep potential well (■: along [100], ▲: along [0$\bar{1}$0]).

the sum ($U_3^+ + U_2^+$) by only 73.5 meV. The total energy of starting entities (−5208 meV) corresponds to an infinite dilution of monomers that is taken as the initial state. Attempts to displace one of the monomers from the closest configuration by successive increments of $a$, along [100] as well as [010] directions, lead to approximately 200 and 50 meV energy barriers, respectively (Figure 8).

Thus, once formed, such a dimer entity cannot spontaneously dissociate; the two doping charges are attracted to each other by means of their excitonic surrounding "glue".

This doping hole pair may constitute the basis of a Cooper pair and lead to Bose condensation. Figure 8 shows that the distance between doping holes, initially of 6.5 Å $\sim a\sqrt{10}/2$, can reach values up to $a\sqrt{34}/2$, according to our remark in section 2.2.1. Larger distances can be obtained by considering, for example, $U_3^+$-$U_3^+$ ESHs. Such values agree well with experimental values for coherence length $\xi$.

**3.2. Double Chains: U-Type Dimers. 3.2.1. Narrow U-Dimers $[U_{nn}^+]_2$.** U-type monomers can be considered as "bidentate exciton ligands" and correspond to strong charge-exciton interactions $\varepsilon_n^+$, as described in Table 2 and discussed in section 2.2.2. In addition, monomers attract each other with interaction energy $\varepsilon^{+2}$ as showed in Figure 9 ($\varepsilon^{+2} = -110$ meV for the $[U_{22}^+]_2$ dimer and $\varepsilon^{+2} = -163$ meV for $[U_{33}^+]_2$).

Once again, as for the T-type dimers, attempts to separate the monomers along [100] as well as [0$\bar{1}$0] lead to high

**Table 3.** Total Energy Gained $U_n^{+2}$ by Exciton-Exciton Plus Charge-Exciton Interaction Energy ($E_T^{+2}$) and Interaction Energy between the Two U-Type Monomers[a]

| | $T_{23}^{+2}$ | $[U_{22}^{+}]_2$ | $[U_{33}^{+}]_2$ | $[U_{1212}^{+}]_2$ |
|---|---|---|---|---|
| $-U_n^{+2}$ | 5134.5 | 7796 | 11863 | 12032 |
| $-E_T^{+2}$ | 1534.5 | 2036 | 3223 | 3392 |
| $\varepsilon_n^{+2}$ | +73.5 | −110 | −163 | −152 |
| $-E_T^{+2}/\sum n$ | 307 | 255 | 269 | 283 |
| $-E_T^{+2}/N_D$ | 128 | 136 | 201 | 136 |
| $N_D$ | 12 | 15 | 21 | 25 |

[a] $\varepsilon_n^{+2}$ are given here as well as the specific $E_T^{+2}$ values per exciton or per $CuO_2$ cell minimum number $N_D$ preserving an isolated dimer character. Energies are in meV.

**Table 4.** Interaction Energy (in meV) between Two Monomers ($U_{22}^{+2}$) Depending on Their Positions along the Chain[a]

| $[U_{22}^{+}]_p$ | N | NN | NNN | NNNN | |
|---|---|---|---|---|---|
| $\varepsilon_{N...N}^{+2}$ | −110 | +78 | +56.5 | +43.5 | |
| $p$ | 2 | 3 | 4 | 5 | 6 |
| $\sum_N \varepsilon_{N...N}^{+2}$ | −110 | −142 | −117.5 | −49.5 | +51.5 |

[a] Nearest (N), next nearest (NN),... (top), and the sum of all $p(p-1)/2$ interactions for a p-oligomer (bottom).

energy barriers, above 200 meV (Figure 9). U-type dimers with $n = 2$ or 3 are thus thermodynamically stable and the two doping charges $h_D^+$ are strongly binded. Table 3 compares their stability with that of the T-type dimer $(T_{23})^{+2}$. Although the sum $E_T^{+2}$ of exciton−exciton ($E_n$), charge-exciton ($\varepsilon_n^+$), and monomer−monomer ($\varepsilon^{+2}$) interactions divided by the number of involved excitons is smaller for U-type ESHs, this ratio increases with $n$.

The ratio $E_T^{+2}/N_D$, where $N_D$ is the minimum number of unit cells preventing direct connections between dimers, favors U-type entities for reasons of compactness.

**3.2.2. Wide U-Dimers $[U_{1212}^{+}]_2$.** For reasons of size and concentration in doping holes, we have restricted our calculations to the case of $[U_{1212}^{+}]_2$ dimers (Table 3).

As for other U-type dimers, the $[U_{1212}^{+}]_2$ dimer formation from the two monomers is thermodynamically favored (−152 meV), with a value $E_T^{+2}/\sum n$ (− 283 meV) close to that of T-type entities. On the reverse, its $E_T^{+2}/N_D$ ratio is more favorable.

In addition, the $[U_{1212}^{+}]_2$ dimer presents the deepest potential well (approximately 235 meV). For these reasons, it appears particularly appropriate to induce strong pairing.

**3.3. $[U_{22}^{+}]_p$ Chain Length.** To evaluate the possible formation of such type of chain, we have calculated not only the interaction energy $\varepsilon_N^{+2}$ between first-neighbor monomers but also between next neighbors ($\varepsilon_{NN}^{+2}$...) (Table 4). Figure 10 illustrates the way energy is gained by building chains of p monomers length.

It is clear that $[U_{22}^{+}]$ monomers cannot constitute long chains, the largest global stability being obtained for $p = 3$. However, plotting $\sum(\varepsilon_{NN}^{+2}/p)$ as a function of $p$ shows that the dimer formation is the most probable ($p = 2$).

We will discuss, in the following, the relationship between such dimers and some checkerboard-type images obtained recently.[13,14]

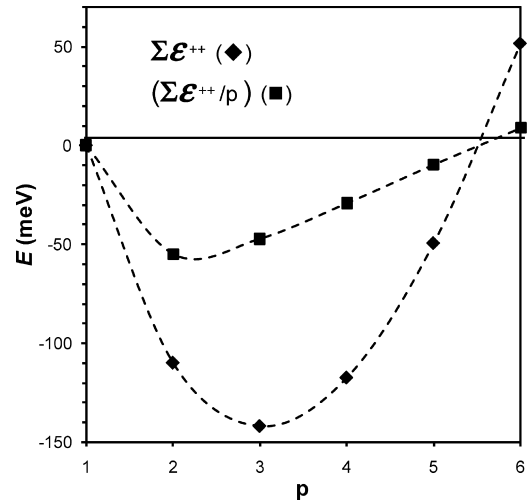


**Figure 10.** Stability of $[U_{22}^{+}]_p$ oligomers, given as $\sum\varepsilon_n^{+2}$ and $(\sum\varepsilon_n^{+2})/p$, as a function of their length $p$.

## 4. Concluding Remarks

As we recently pointed out,[1] exciton formation associating a hole from the top of the LHB with an electron from the bottom of the UHB, when the band gap tends to vanish, can be favored by the occurrence of doping holes in LHB.

We recall that, here, excitons are charge-transfer and Frenkel-type excitons: (i) they locally change the normal ($Cu^{2+}/O^{2-}$) state into another redox state ($Cu^{+}/O^{-}$), that is energetically close, and correspond to an electron−hole quasiparticle; (ii) within an exciton, the distance between the hole and electron charges is approximately 2 Å, a situation that differs strongly from Mott−Wannier excitons found in some semiconductors, with larger size and isotropic character. The induced effective electrical dipole ($e^-$ on Cu and $h^+$ on O) corresponds to a reversal polarization of the $Cu^{2+}-O^{2-}$ bond.

Both characteristics (anisotropy and fixed direction of the electrical dipoles) are necessary to achieve a net attractive interaction between the doping holes.

On the basis of the previously quoted assumptions (low screening by charge carriers and Coulomb forces with significant spatial extent, $k/\varepsilon_r = 0.10$), we have shown the following:

(i) The proposed mechanism is basically different from the ones discussed successively by Little, Ginzburg, Bardeen, Hirsch, Scalapino, Varma and others, that is, an exchange between electrons (or holes) and virtual excitons, as quoted for example by Bardeen:[16] "Effective attractive interaction between electrons comes from virtual excitation of excitons rather than phonons...". The main present criticism against this time-scale retarded mechanism is that such excitations should be accompanied by dynamical distortions, actually involving phonons.

Here, we show that two ESH entities can form thermodynamically stable dimers, bringing a "pairing glue" in real

(16) Allender, D.; Bray, J.; Bardeen, J. *Phys. Rev. B* **1973**, *7*, 1020.

space, and that trimer entities should be less stable. Thus, it is a non-retarded mechanism, with a much shorter time-scale than phonon-assisted mechanisms.

(ii) Our model agrees well with the phase diagram (Figure 6) defining under-doped, overdoped, and optimized compositions in high-$T_C$ cuprates:

- as doping holes bring large interaction energies with excitons, they contribute to the formation of the ESH excitonic surrounding, above a critical $x_0$ value close to 0.05,

- optimizing the specific total interaction energy $E_T{}^{+2}/N_D$ corresponds to $x_c$ values between 10 and 14%,

- overdoping induces a too low ratio of excitons per doping hole, and small ESHs unfavorable to link monomers into dimers. In addition, increase of covalency and collapse of the LHB-UHB gap lead to a normal Fermi-liquid behavior.

(iii) Our model is consistent with a coherence length of nearly 10 Å.

(iv) It agrees well with the recently published images by Kohsaka et al.,[14] obtained by atomic-resolution tunnelling-assymmetry spectroscopy on lightly doped $Ca_{2-x}Na_xCuO_2Cl_2$ samples, showing that hole carriers are non-homogeneously distributed on some rows of oxygen atoms, according to a 4 $\times$ $a$ superstructure. Hole repartition draws a ladder-type feature, with a rung periodicity of $a$. If we keep in mind that such images are time-averaged during the variable bias application, they can be explained by the $[U_{1212}{}^{+}]_p$ ESHs displacement. Such kind of gliding can be induced by reversible Cu−O bond polarization, as well as by free displacement of the exciton cloud.

(v) This model suggests explanations for some peculiarities of $CuO_2$ planes and their Fermi surface, that is, their gapped behavior along $(0,\pi)$ directions (which is that of the pair displacement as described for U-type ESHs), and hole pockets along the $(\pi,\pi)$ direction, where the remaining unpaired doping holes can move in rows of oxygen atoms along [110], as schematized in Figure 11.

All quantities given here have only comparative significance because they depend of the chosen value of the $k/\varepsilon_r$ parameter.

(vi) Finally, this model may also apply to the recently discovered LnOFeAs electron-doped superconductors.[17,18]

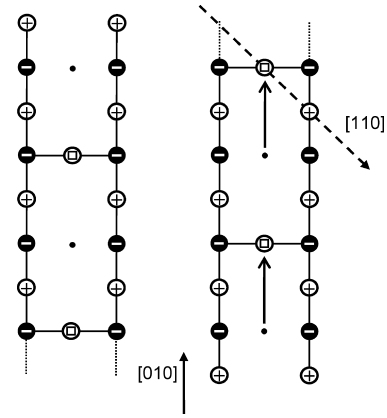


**Figure 11.** $[U_{22}{}^{+}]_2$ dimer showing the possible [010] pair gliding (corresponding to a gapped behavior in the Brillouin zone along *X*- or *Y*-direction), and the gliding of single holes ($\sigma^*$ $b_{1g}$(O−Cu) band) into the [110] rows of oxygen atoms.

The Fe−As system is well-known for charge transfer phenomena as, for example, in the marcassite-type structure ($FeAs_2$).

By showing the ESH dimer thermodynamic stability, this paper brings arguments for the issue: "...whether pairing is a low-energy instability in which quasi particles are bound into Copper pairs (as in BCS theory), or if it is instead a fundamental property of the doped Mott−Hubbard insulating state", as questioned by Orenstein and Millis.[19] This constitutes a new category of superconductivity mechanisms with local non-retarded attractive interactions.[20]

**Acknowledgment.** One of us (M.P.) thanks Jacques Friedel and Philippe Nozières for fruitful discussions.

IC801266Q

(17) Kamihara, Y.; Watanabe, T.; Hirano, M.; Hosono, H. *J. Am. Chem. Soc.* **2008**, *130*, 3296.
(18) Ren, Z. A.; Che, G. C., Dong, X. L.; Yang, J.; Lu, W.; Yi, W.; Shen X. L.; Li, Z. C.; Sun, L. L.; Zhou F.; Zhao Z. X. cond-mat/arXiv: 0804.2582v1.
(19) Orenstein, J.; Millis, A. J. *Science* **2000**, *288*, 468.
(20) Micnas, R.; Ranninger, J.; Robaszkiewicz, S. *Rev. Mod. Phys.* **1990**, *62*, 113.